

Supporting Information

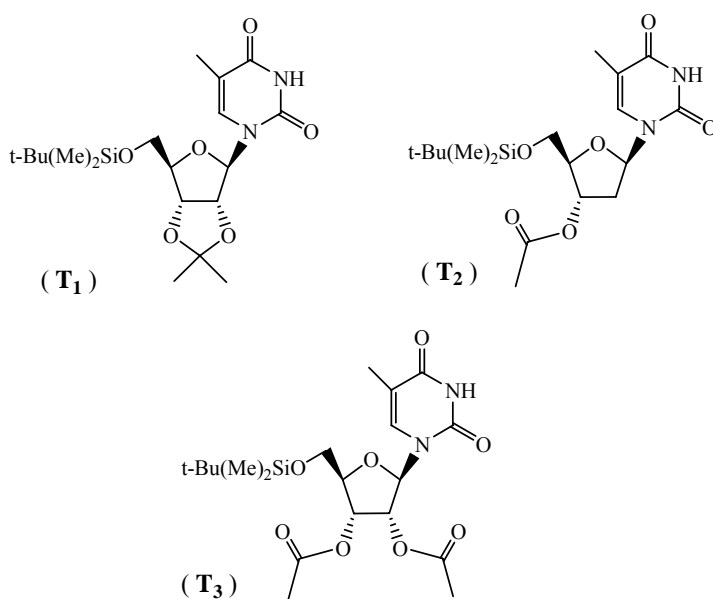
The formation of thymidine-based T-tetramers with remarkable structural and metal ion size effects

Qun Luo, Dayong Wu, Shixiong Liu, Daihua Tang, Yong Huang, Xinhou Liu,
Fuyi Wang, Ruiyao Wang and Gang Wu

Table of Contents

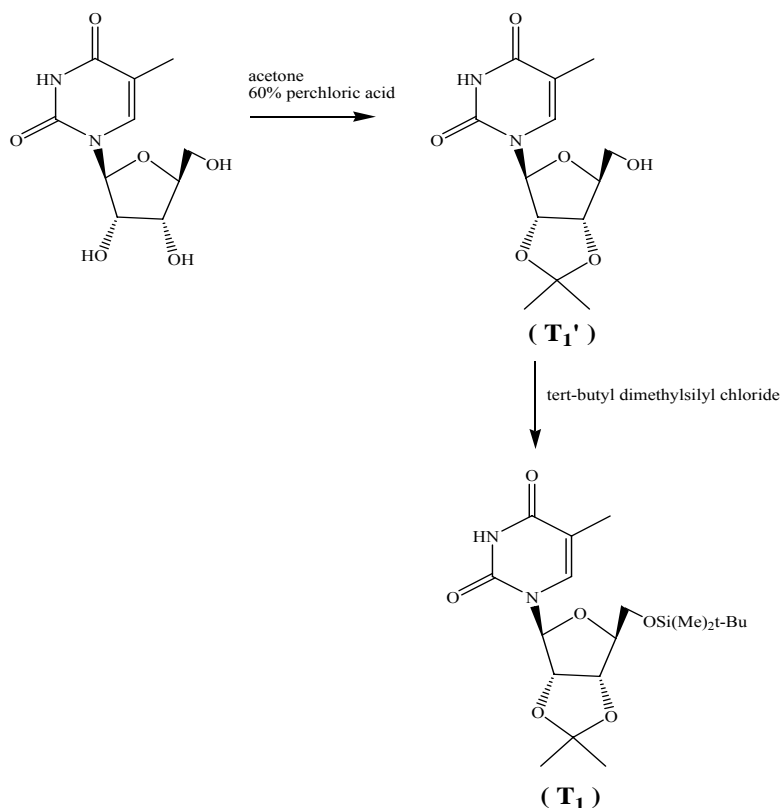
Scheme S1. Chemical structures for T ₁ , T ₂ and T ₃	2
Synthesis of T ₁	3
Figure S1. ¹ H NMR spectrum of T ₁ in CDCl ₃ at 298 K	4
Figure S2. ¹ H NMR spectrum of T ₁ in CD ₃ CN at 298 K	4
Figure S3. ¹³ C NMR spectrum of T ₁ in CDCl ₃ at 298 K	5
Synthesis of T ₂	5
Figure S4. ¹ H NMR spectrum of T ₂ ' in CDCl ₃ at 298 K	7
Figure S5. ¹³ C NMR spectrum of T ₂ ' in CDCl ₃ at 298 K	7
Figure S6. ¹ H NMR spectrum of T ₂ in CDCl ₃ at 298 K	8
Figure S7. ¹³ C NMR spectrum of T ₂ in CDCl ₃ at 298 K	8
Synthesis of T ₃	9
Figure S8. ¹ H NMR spectrum of T ₃ ' in CDCl ₃ at 298 K	10
Figure S9. ¹³ C NMR spectrum of T ₃ ' in CDCl ₃ at 298 K	11
Figure S10. ¹ H NMR spectrum of T ₃ in CDCl ₃ at 298 K	11
Figure S11. ¹³ C NMR spectrum of T ₃ in CDCl ₃ at 298 K	12
X-ray crystallographic analysis for T ₂	12
Figure S12. ESI-MS of T ₂ -NaCl in CH ₃ CN	13
Table S1. Signal assignment of TOF-ESI-MS for a mixture of T ₁ and alkali metal chloride in acetonitrile	14
Figure S13. Comparison between experimental result and simulated isotopic pattern for TOF-ESI-MS of T ₁ +Na ⁺ ion	15
Figure S14. Comparison between experimental result and simulated isotopic pattern for TOF-ESI-MS of 2 T ₁ +Na ⁺ ion	15

Figure S15. Comparison between experimental result and simulated isotopic pattern for TOF-ESI-MS of $3\mathbf{T}_1+\text{Na}^+$ ion	16
Figure S16. Comparison between experimental results and simulated isotopic patterns for TOF-ESI-MS of $4\mathbf{T}_1+\text{Na}^+$ monomer and $4\mathbf{T}_1+\text{Na}^+$ dimer	16
Figure S17. Comparison between experimental results and simulated isotopic patterns for TOF-ESI-MS of $4\mathbf{T}_1+\text{K}^+$ monomer and $4\mathbf{T}_1+\text{K}^+$ dimer	17
Figure S18. Comparison between experimental results and simulated isotopic patterns for TOF-ESI-MS of $4\mathbf{T}_1+\text{Rb}^+$ monomer and $4\mathbf{T}_1+\text{Rb}^+$ dimer	17
Figure S19. Comparison between experimental results and simulated isotopic patterns for TOF-ESI-MS of $5\mathbf{T}_1+\text{Rb}^+$ monomer and $5\mathbf{T}_1+\text{Rb}^+$ dimer	18
Figure S20. Comparison between experimental result and simulated isotopic pattern for TOF-ESI-MS of $[4\mathbf{T}_1+\text{Rb}^+]+[5\mathbf{T}_1+\text{Rb}^+]$ ion	18
Figure S21. Comparison between experimental results and simulated isotopic patterns for TOF-ESI-MS of $4\mathbf{T}_1+\text{Cs}^+$ monomer and $4\mathbf{T}_1+\text{Cs}^+$ dimer	19
Figure S22. Comparison between experimental results and simulated isotopic patterns for TOF-ESI-MS of $5\mathbf{T}_1+\text{Cs}^+$ monomer and $5\mathbf{T}_1+\text{Cs}^+$ dimer	19
Figure S23. Comparison between experimental result and simulated isotopic pattern for TOF-ESI-MS of $[4\mathbf{T}_1+\text{Cs}^+]+[5\mathbf{T}_1+\text{Cs}^+]$ ion	20
Figure S24. Positive ion-mode TOF-ESI-MS sections for \mathbf{T}_1 -pentamers and dimeric \mathbf{T}_1 -pentamers in acetonitrile	20



Scheme S1. Chemical structures for \mathbf{T}_1 , \mathbf{T}_2 and \mathbf{T}_3

Synthesis of **T**₁



Synthesis of **T**₁ was achieved according to the similar procedures.^{1,2}

The mixture of 5-methyluridine (981 mg, 3.8 mmol), 60% perchloric acid (0.1 mL) and acetone (40 mL) was stirred at room temperature for 3 h. To it was added ammonium hydroxide till the solution was neutral. Chromatography (97:3 CH₂Cl₂:MeOH) gave the product as a white solid (0.95 g). ESI-MS (**T**₁' + Na⁺): 321.2 (base peak) (calcd. 321.1). The solid product was mixed with imidazole (435 mg, 6.4 mmol) in methylene chloride (35 mL), and to it was added tert-butyl dimethylsilyl chloride (722 g, 4.8 mmol). The reaction mixture was stirred at room temperature for 12 h, after which time TLC analysis indicated the reaction was complete. The reaction mixture was washed with 0.01 N HCl, saturated NaHCO₃, and saturated NaCl. Chromatography (98:2 CH₂Cl₂:MeOH) gave **T**₁ as a colorless soft matter (1.136 g, 2.8 mmol) and the yield was 72% based on the starting material (5-methyluridine). ¹H NMR (500 MHz, CDCl₃) δ 9.64 (s, 1 H, H3), 7.29 (s, 1 H, H6), 5.91 (d, 1 H, J = 2.46 Hz, H1'), 4.75 (m, 1 H, J = 3.10, 6.62 Hz, H2'), 4.73 (m, 1 H, J = 2.99, 6.20 Hz, H3'), 4.25 (m, 1 H, J = 2.89 Hz, H4'), 3.90 (dd, 1 H, J = 2.67, 11.43 Hz, H5'), 3.80 (dd, 1 H, J = 3.53, 11.43 Hz, H5''), 1.90 (s, 3 H, CH₃), 1.58 (s, 3 H, CH₃), 1.34 (s, 3 H, CH₃), 0.90 (s, 9 H, t-Bu), 0.0864 (s, 3 H, Si(CH₃)), 0.07956 (s, 3 H, Si(CH₃)). ¹³C NMR (500 MHz, CDCl₃) δ 164.58, 150.80, 136.81, 114.60, 111.16, 92.27, 86.55, 85.10, 80.78, 63.71, 27.66, 26.30, 25.77, 18.77, 12.87, -4.94, -5.024.

Anal. Calcd for C₁₉H₃₂N₂O₆Si. C, 55.32; H, 7.82; N, 6.79. Found: C, 54.95; H, 7.96; N, 6.65.

References

[1] A. Hampton, *J. Am. Chem. Soc.*, 1961, **83**, 3640-3645.

- [2] S. L. Forman, J. C. Fetting, S. Pieraccini, G. Gottarelli and J. T. Davis, *J. Am. Chem. Soc.*, 2000, **122**, 4060-4067.

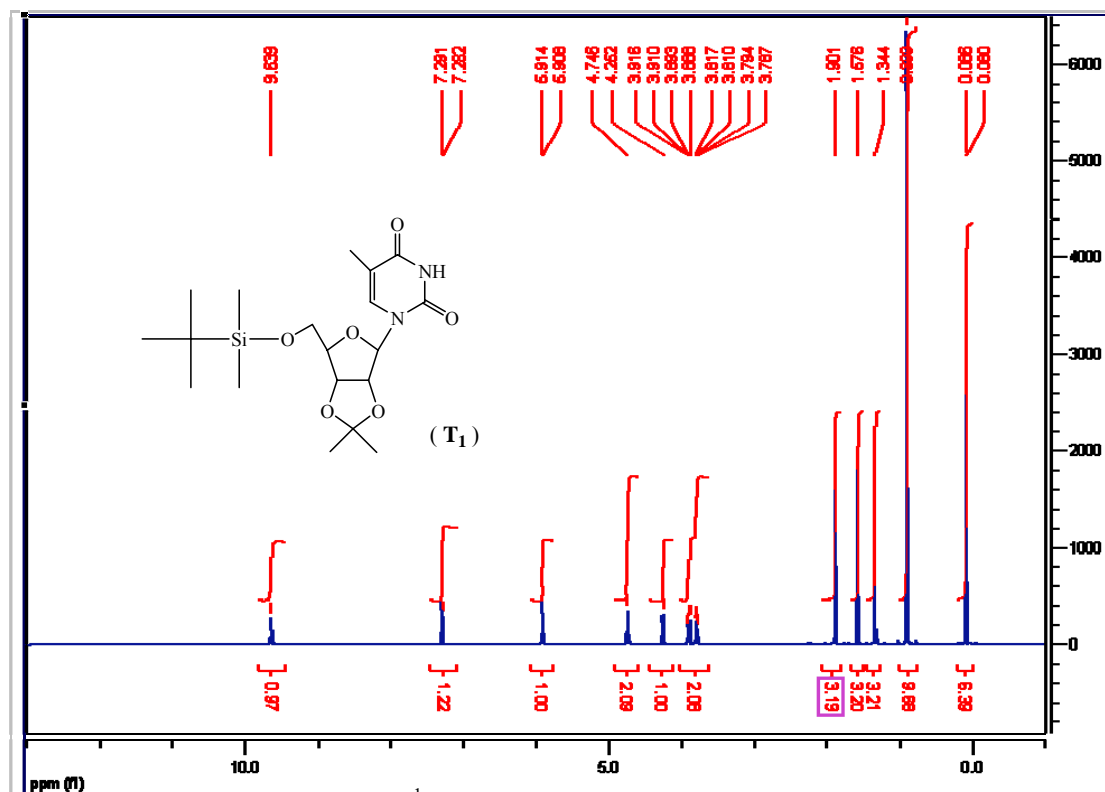


Figure S1. ^1H NMR spectrum of T_1 in CDCl_3 at 298 K

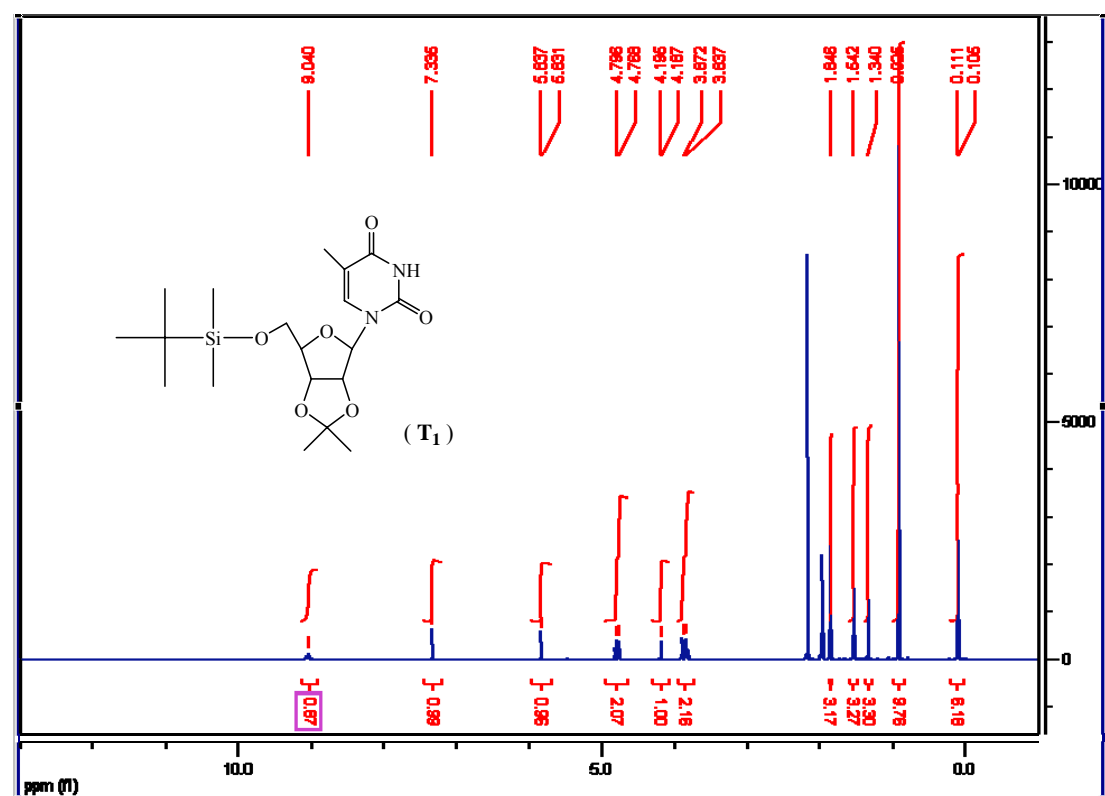


Figure S2. ^1H NMR spectrum of T_1 in CD_3CN at 298 K

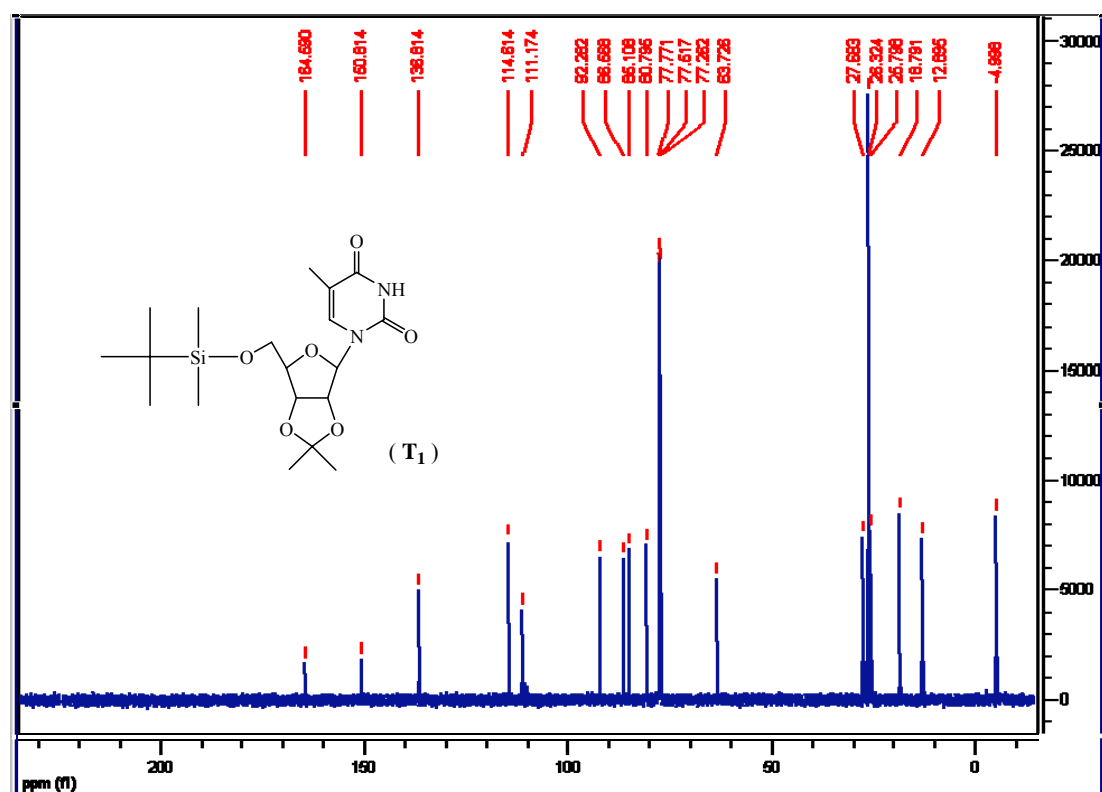
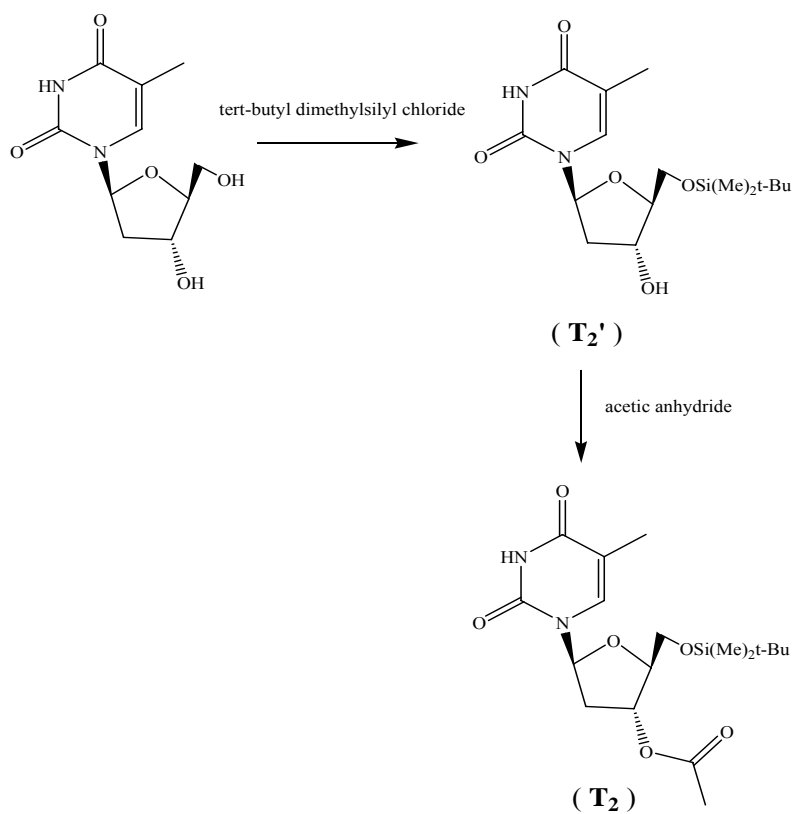


Figure S3. ¹³C NMR spectrum of **T₁** in CDCl₃ at 298 K

Synthesis of **T₂**



Synthesis of **T₂** was achieved according to the similar procedures.¹

Synthesis of **T₂'**

To a suspension of thymidine (968 g, 4 mmol) and imidazole (544 mg, 8 mmol) in methylene chloride (50 mL) was added tert-butyl dimethylsilyl chloride (602 g, 4 mmol). The reaction mixture was stirred at room temperature for 24 h, after which time TLC analysis indicated the reaction was complete. The reaction mixture was washed with 0.01 N HCl, saturated NaHCO₃, and saturated NaCl. Chromatography (25:1 CH₂Cl₂:CH₃OH) gave **T₂'** as a colorless solid (345 mg, 24.2%). M.p.: 196-197 °C. ESI-MS (**T₂'**+Na⁺) 379.3 (base peak) (calcd. 379.2). ¹H NMR (400 MHz, CDCl₃) δ 9.57 (s, 1 H, H3), 7.54 (m, 1 H, J = 1.18 Hz, H6), 6.39 (dd, 1 H, J = 5.68, 8.07 Hz, H1'), 4.44 (d, 1 H, J = 5.50 Hz), 4.06 (m, 1 H, J = 2.02 Hz), 3.87 (m, 2 H, J = 2.02, 11.37 Hz), 3.25 (s, broad, OH), 2.38 (m, 1 H, J = 5.87, 13.39 Hz), 2.07 (m, 1 H, J = 6.05, 8.25 Hz), 1.90 (s, 3 H, CH₃), 0.90 (s, 9 H, t-Bu), 0.10 (d, 6 H, J = 2.93 Hz, Si(CH₃)₂). ¹³C NMR (400 MHz, CDCl₃) δ 164.2, 150.8, 135.7, 111.1, 87.5, 85.2, 72.7, 63.8, 41.3, 26.1, 18.5, 12.7, 0.1, -5.2, -5.3.

Anal. Calcd for C₁₆H₂₈N₂O₅Si: C, 53.91; H, 7.92; N, 7.86. Found: C, 54.41; H, 7.95; N, 7.89.

Synthesis of **T₂**

The mixture of **T₂'** (178 mg, 0.5 mmol), acetic anhydride (10 mL) and pyridine (1 mL) was stirred at room temperature for 15 h. To it was added water (50 mL) and the resultant suspension was filtered. Chromatography (98:2 CH₂Cl₂:CH₃OH) gave **T₂** as a white solid (130 mg, 65%). M.p.: 141-142 °C. ¹H NMR (500 MHz, CDCl₃) δ 9.36 (s, 1 H, H3), 7.55 (m, 1 H, J = 1.18 Hz, H6), 6.38 (dd, 1 H, J = 5.24, 9.30 Hz, H1'), 5.25 (d, 1 H, J = 5.98 Hz, H3'), 4.10 (m, 1 H, J = 1.39 Hz, H4'), 3.92 (m, 2 H, J = 1.82 Hz, H5', H5''), 2.41 (dd, 1 H, J = 5.24, 13.68 Hz, H2'), 2.12 (m, 1 H, H2''), 2.11 (s, 3 H, CH₃), 1.93 (s, 3 H, CH₃), 0.94 (s, 9 H, t-Bu), 0.14 (s, 6 H, Si(CH₃)₂). ¹³C NMR (500 MHz, CDCl₃) δ 171.04, 164.25, 150.98, 135.41, 111.68, 85.77, 85.08, 75.81, 64.00, 38.40, 26.32, 21.42, 18.73, 12.91, -4.986, -5.093.

Anal. Calcd for C₁₈H₃₀N₂O₆Si: C, 54.25; H, 7.59; N, 7.03. Found: C, 54.34; H, 7.81; N, 6.90.

Reference

[1] S. Wendicke, S. Warnecke and C. Meier, *Angew. Chem. Int. Ed.*, 2008, **47**, 1500-1502.

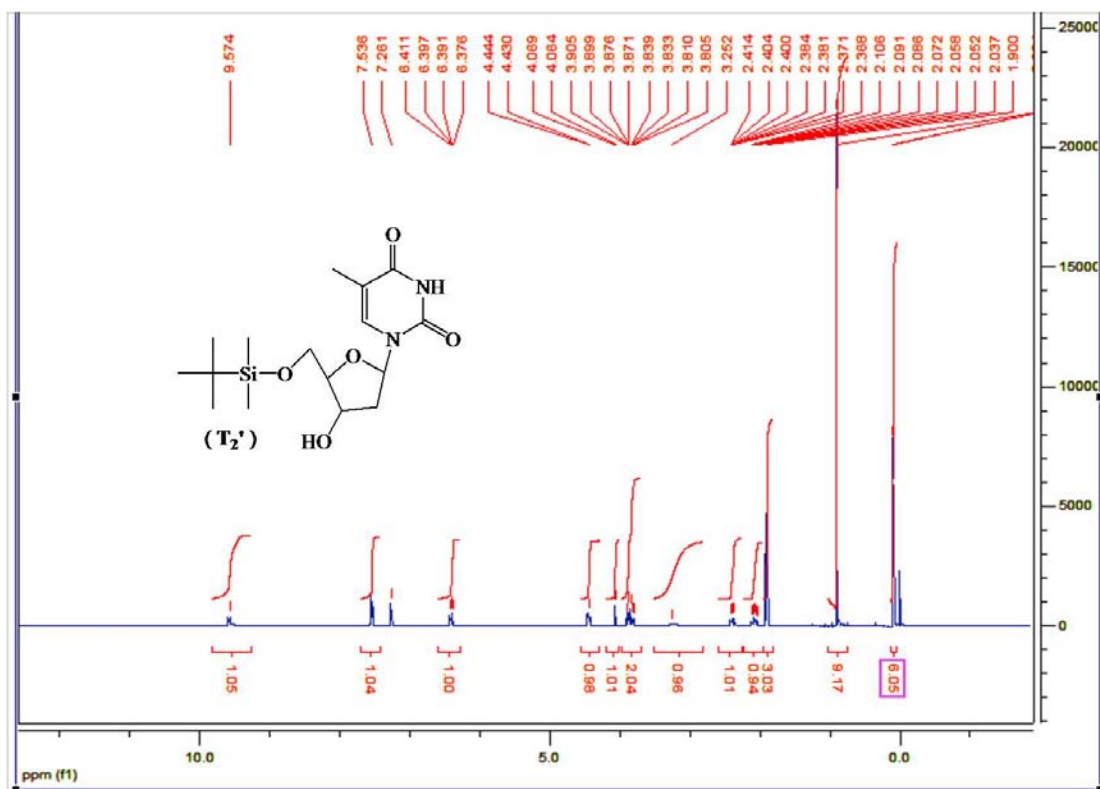


Figure S4. 1H NMR spectrum of T_2' in $CDCl_3$ at 298 K

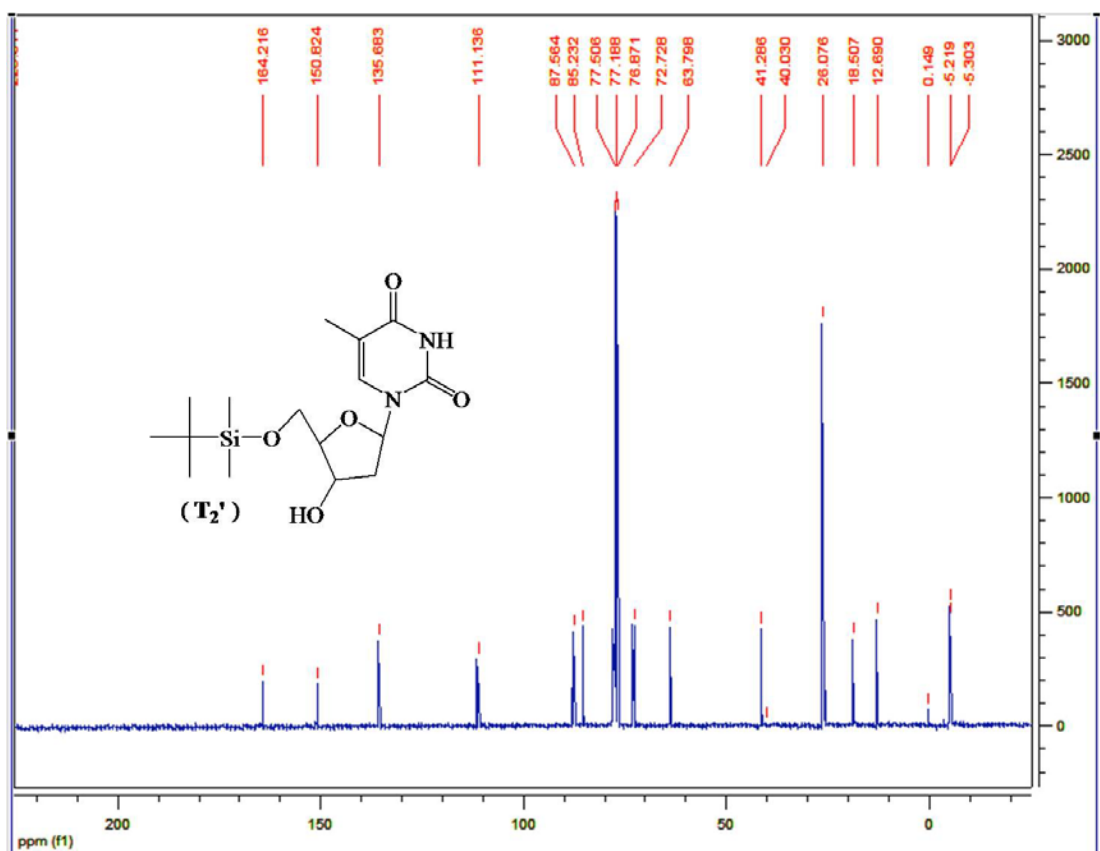


Figure S5. ^{13}C NMR spectrum of T_2' in $CDCl_3$ at 298 K

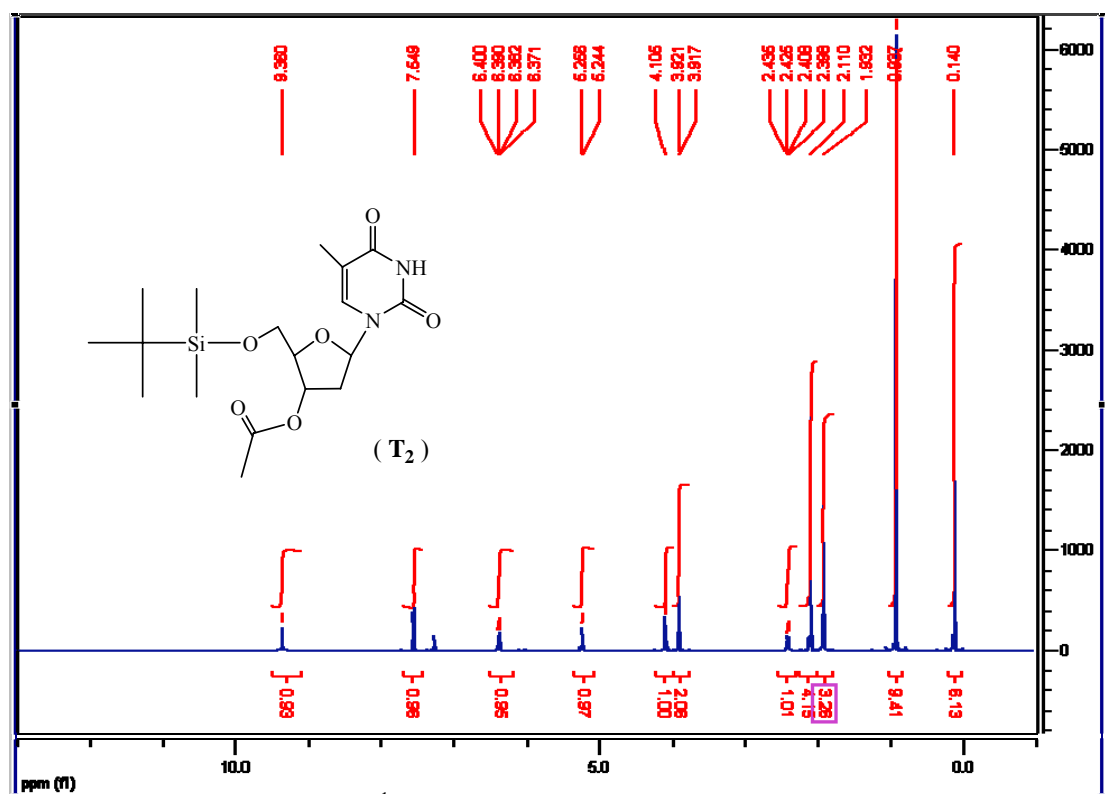


Figure S6. 1H NMR spectrum of T_2 in $CDCl_3$ at 298 K

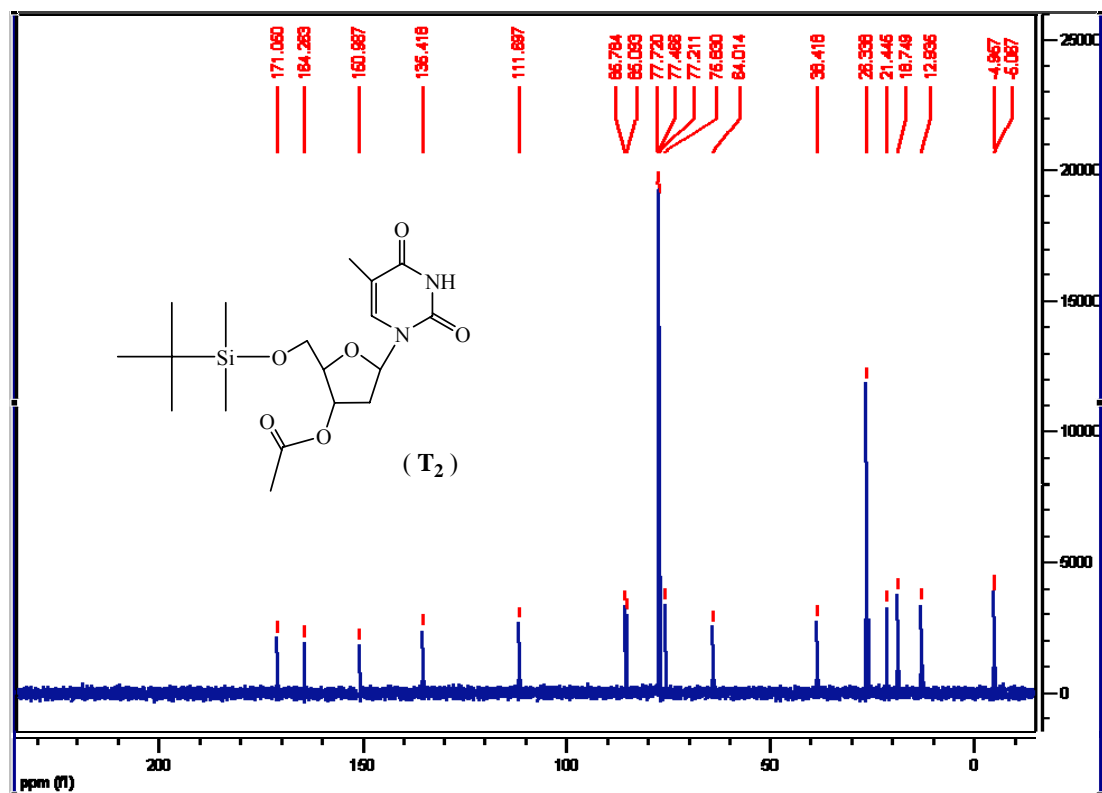
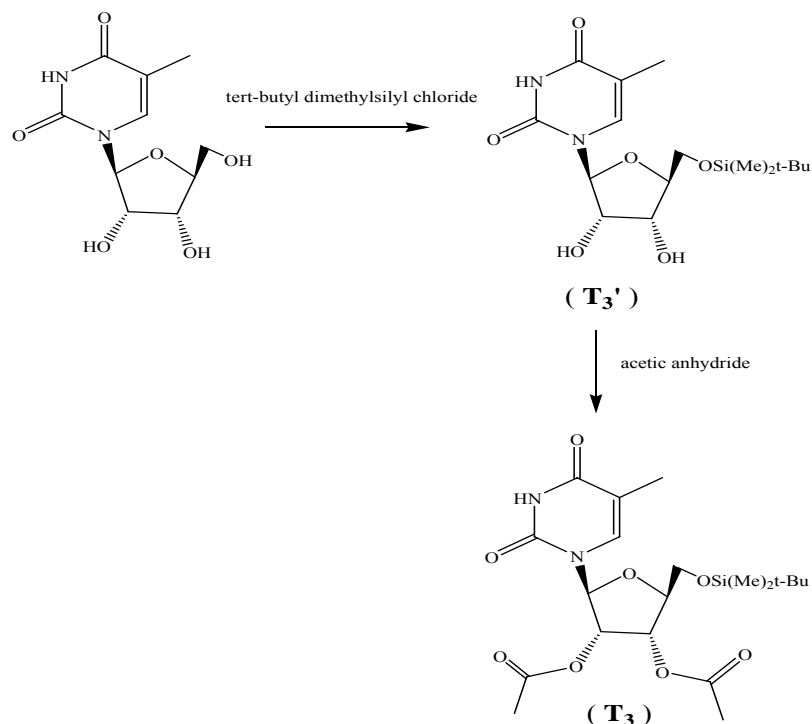


Figure S7. ^{13}C NMR spectrum of T_2 in $CDCl_3$ at 298 K

Synthesis of **T₃**



Synthesis of **T₃** was achieved according to the similar procedures.¹

Synthesis of **T₃'**

To a suspension of 5-methyluridine (1032 mg, 4 mmol) and imidazole (544 mg, 8 mmol) in methylene chloride (50 mL) was added tert-butyl dimethylsilyl chloride (602 g, 4 mmol). The reaction mixture was stirred at room temperature for 48 h, after which time TLC analysis indicated the reaction was complete. The reaction mixture was washed with 0.01 N HCl, saturated NaHCO₃, and saturated NaCl. Chromatography (25:1 CH₂Cl₂:MeOH) gave **T₃'** as a colorless solid (744 mg, 50 %). M.p.: 210-211 °C. ESI-MS (**T₃'**+Na⁺) 395.3 (calcd. 395.2). ¹H NMR (400 MHz, CDCl₃) δ 9.54 (s, 1 H, H3), 7.59 (m, 1 H, J = 1.10 Hz, H6), 5.86 (d, 1 H, J = 3.85 Hz, H1'), 4.23 (m, 3 H, H2', H3', H4'), 3.95 (dd, 2 H, J = 10.82, 56.49 Hz, H5', H5''), 1.90 (m, 3 H, J = 0.73 Hz, CH₃), 0.90 (s, 9 H, t-Bu), 0.10 (s, 3 H, Si(CH₃)₂). ¹³C NMR (400 Hz, CDCl₃) δ 164.0, 151.6, 135.7, 110.7, 90.8, 86.3, 71.3, 63.0, 26.0, 18.5, 12.7, 0.1, -5.3.

Anal. Calcd for C₁₆H₂₈N₂O₆Si: C, 51.59; H, 7.58; N, 7.52. Found: C, 52.05; H, 7.61; N, 7.56.

Synthesis of **T₃**

The mixture of **T₃'** (186 mg, 0.5 mmol), acetic anhydride (10 mL) and pyridine (1 mL) was stirred at room temperature for 15 h. To it was added water (50 mL) and the resultant suspension was filtered. Chromatography (98:2 CH₂Cl₂:CH₃OH) gave **T₃** as a white solid (142 mg, 62%).

M.p.: 133-134 °C. ESI-MS ($T_1'^+Na^+$) 321.2 (calcd. 321.1). 1H NMR (500 MHz, $CDCl_3$) δ 9.41 (s, 1 H, H3), 7.49 (m, 1 H, $J = 1.07$ Hz, H6), 6.33 (d, 1 H, $J = 7.69$ Hz, H1'), 5.35 (dd, 1 H, $J = 1.50$, 5.45 Hz, H2'), 5.28 (dd, 1 H, $J = 5.56$, 7.69 Hz, H3'), 4.19 (m, 1 H, $J = 1.71$ Hz, H4'), 3.92 (dd, 1 H, $J = 1.71$, 11.43 Hz, H5'), 3.86 (dd, 1 H, $J = 1.82$, 11.54 Hz, H5''), 2.15 (s, 3 H, CH_3), 2.07 (s, 3 H, CH_3), 1.93 (s, 3 H, CH_3), 0.97 (s, 9 H, t-Bu), 0.17487 (s, 3 H, $Si(CH_3)$), 0.16696 (s, 3 H, $Si(CH_3)$). ^{13}C NMR (500 Hz, $CDCl_3$) δ 170.46, 170.15, 164.10, 151.30, 135.06, 112.33, 84.87, 84.09, 73.13, 72.20, 63.68, 26.32, 21.15, 20.83, 18.75, 12.87, -5.054, -5.093.

Anal. Calcd for $C_{20}H_{32}N_2O_8Si$: C, 52.61; H, 7.06; N, 6.14. Found: C, 52.82; H, 7.11; N, 6.29.

Reference

[1] S. Wendicke, S. Warnecke and C. Meier, *Angew. Chem. Int. Ed.*, 2008, **47**, 1500-1502.

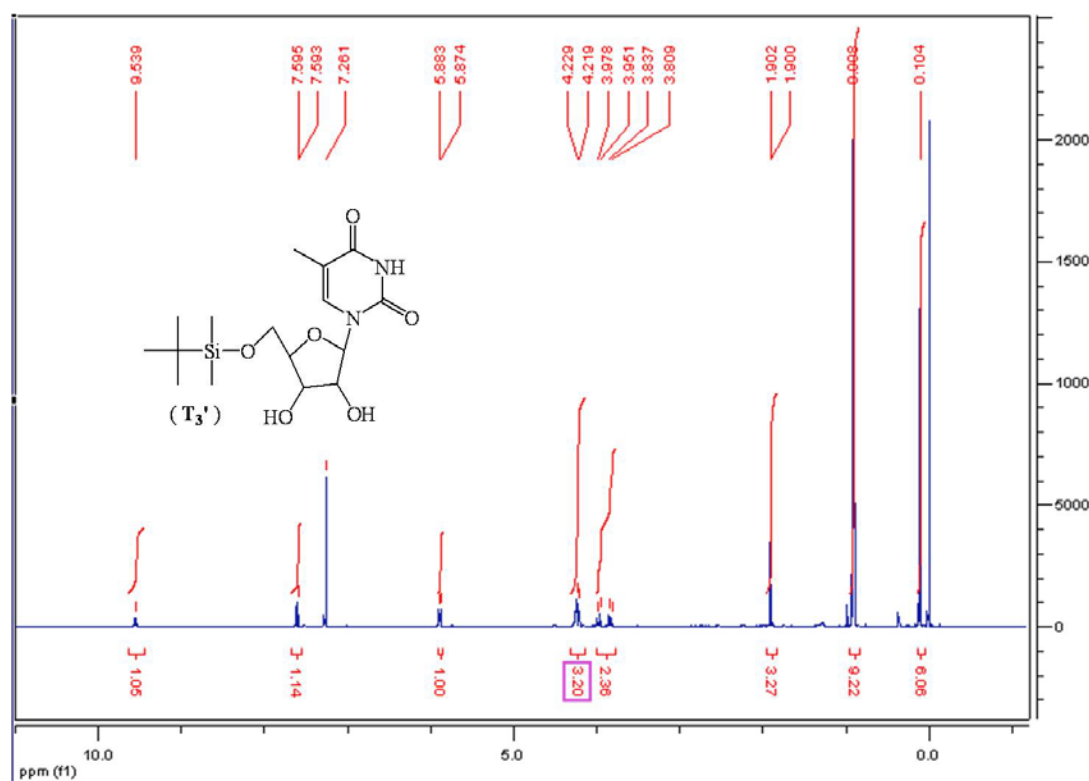


Figure S8. 1H NMR spectrum of T_3' in $CDCl_3$ at 298 K

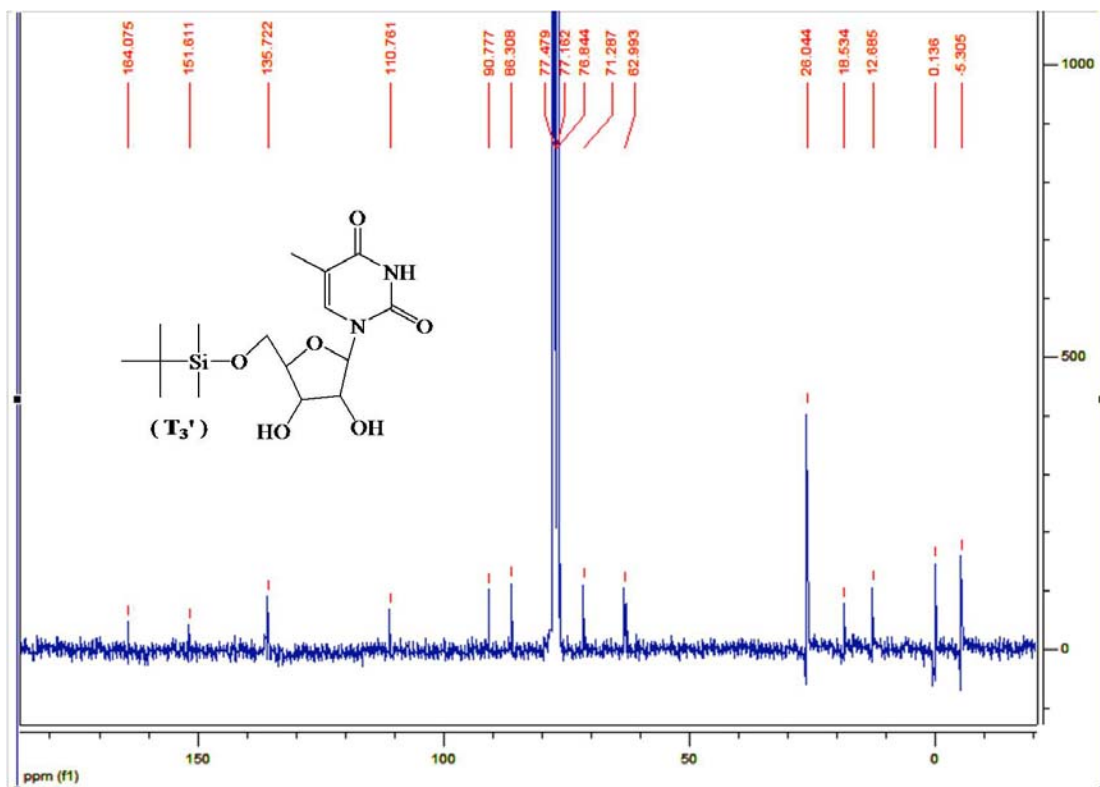


Figure S9. ^{13}C NMR spectrum of T_3' in CDCl_3 at 298 K

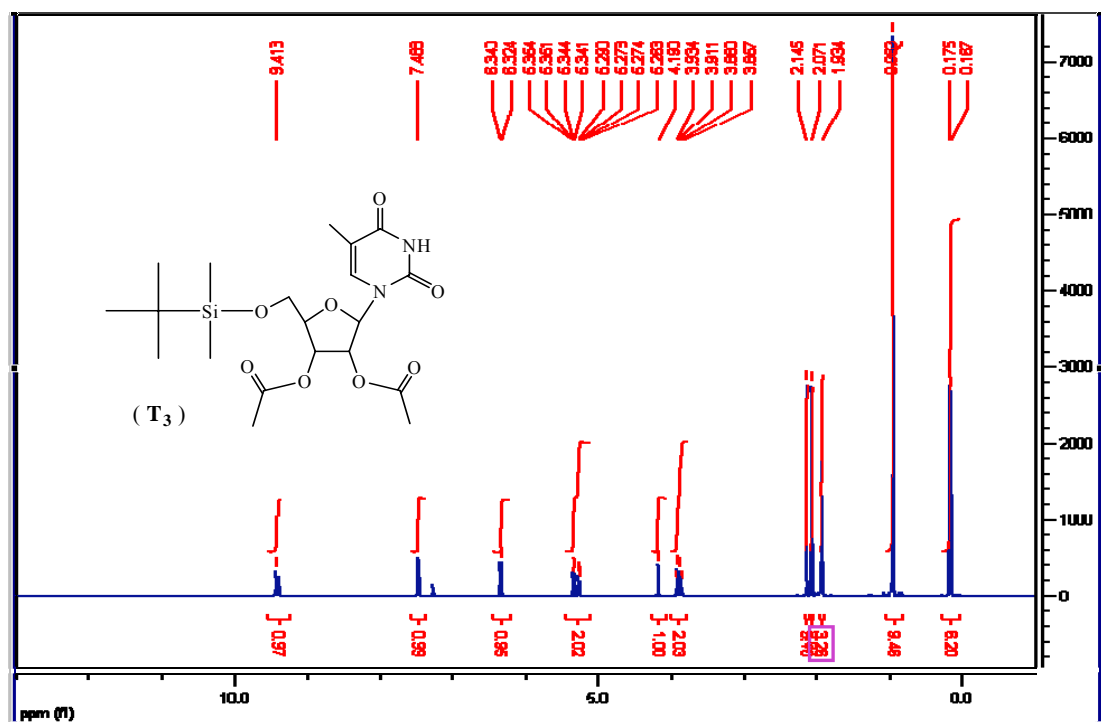


Figure S10. ^1H NMR spectrum of T_3 in CDCl_3 at 298 K

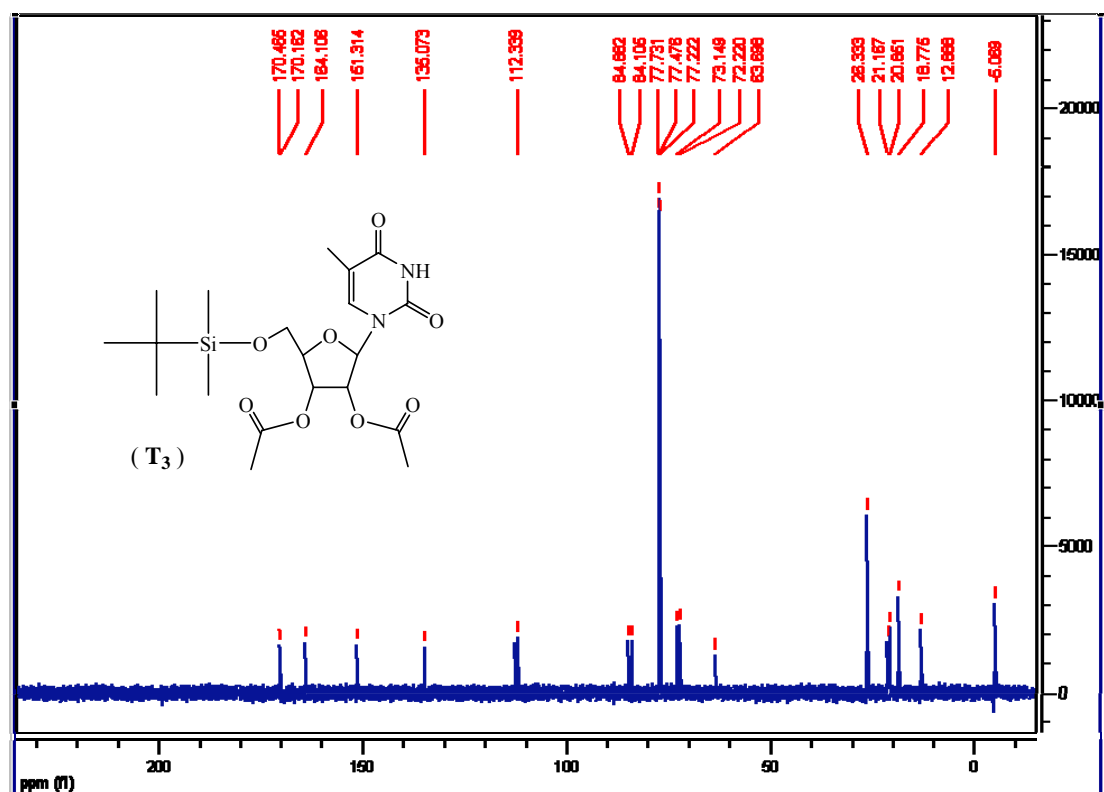


Figure S11. ¹³C NMR spectrum of **T₃** in CDCl₃ at 298 K

X-ray Crystallographic Analysis for **T₂**

A crystal of **T₂** (colorless, block-shaped, size 0.5 x 0.5 x 0.2mm) was mounted on a glass fiber with grease very quickly. Data collection was performed on a Bruker SMART CCD 1000 X-ray diffractometer with graphite-monochromated Mo K radiation ($\lambda = 0.71073 \text{ \AA}$), operating at 50 kV and 30 mA over 2 ranges of $2.60 \sim 52.00^\circ$ at -93°C controlled with Crysostream Controller 700. No significant decay was observed during the data collection.

Data were processed on a Pentium PC using the Bruker AXS Windows NT software package (version 5.10).¹ Neutral atom scattering factors were taken from Cromer and Waber.² The raw intensity data were converted (including corrections for scan speed, background, and Lorentz and polarization effects) to structure amplitudes and their esd's using the program SAINT-Plus, which corrects for L_p and decay. Empirical absorption corrections were applied using program SADABS. The structure is solved and refined by using SHELXTL. The crystal is orthorhombic space group $C22_1$, based on the systematic absences, E statistics and successful refinement of the structure. The structure was solved by direct methods. Full-matrix least-square refinements minimizing the function $\sum w (F_o^2 - F_c^2)^2$ were applied to the compound. All non-hydrogen atoms were refined anisotropically. Most of the hydrogen atoms were located gradually from the difference Fourier

map and their contributions were included in the structure factor calculations. Convergence to final $R_1 = 0.0266$ and $wR_2 = 0.0660$ by using 3647 ($I > 2\sigma(I)$) independent reflections and 340 parameters were achieved,³ with the largest residual peak and hole to be 0.177 and $-0.167 \text{ e}/\text{\AA}^3$, respectively.

-
- [1] Bruker AXS Crystal Structure Analysis Package, Version 5.10 (SMART NT (Version 5.053), SAINT-Plus (Version 6.01), SHELXTL (Version 5.1)); Bruker AXS Inc.: Madison, WI, 1999.
- [2] D. T. Cromer and J. T. Waber, *Interactional Tables for X-ray Crystallography*; Kynoch Press: Birmingham, UK, 1974; Vol. 4, Table 2.2 A.
- [3] $R_1 = \sum ||Fo| - |Fc|| / \sum |Fo|$
 $wR_2 = \{\sum [w(Fo^2 - Fc^2)^2] / \sum [w(Fo^2)^2]\}^{1/2}$
 $(w = 1 / [\sigma^2(Fo^2) + (0.0447P)^2], \text{ where } P = [\text{Max}(Fo^2, 0) + 2Fc^2] / 3)$

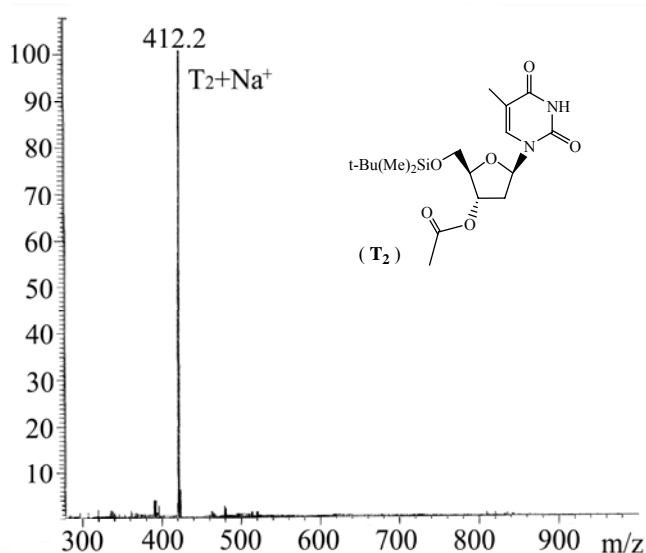


Figure S12. ESI-MS of T_2 -NaCl in acetonitrile

Table S1. Signal assignment of TOF-ESI-MS for a mixture of **T**₁ and alkali metal chloride in acetonitrile

TOF-ESI-MS peaks	Experimental value	Calculated value
T ₁ +Li ⁺	419.6	419.2
2 T ₁ +Li ⁺	831.2	831.4
3 T ₁ +Li ⁺	1242.6	1243.6
T ₁ +Na ⁺	435.6	435.2
2 T ₁ +Na ⁺	847.1	847.4
3 T ₁ +Na ⁺	1258.4	1259.6
4 T ₁ +Na ⁺ (T ₁ -tetramer)	1670.7	1672.8
[4 T ₁ +Na ⁺] ₂ (dimeric T ₁ -tetramers)	1670.7	1672.8
T ₁ +K ⁺	451.2	451.2
2 T ₁ +K ⁺	863.1	863.4
3 T ₁ +K ⁺	1274.4	1275.6
4 T ₁ +K ⁺ (T ₁ -tetramer)	1686.7	1688.8
[4 T ₁ +K ⁺] ₂ (dimeric T ₁ -tetramers)	1686.7	1688.8
T ₁ +Rb ⁺	497.4	497.1
2 T ₁ +Rb ⁺	909.0	909.3
[2 T ₁ +Rb ⁺]+[3 T ₁ +Rb ⁺]	1115.7	1116.4
3 T ₁ +Rb ⁺	1321.3	1322.5
[3 T ₁ +Rb ⁺]+[4 T ₁ +Rb ⁺]	1527.5	1529.1
4 T ₁ +Rb ⁺ (T ₁ -tetramer)	1733.6	1735.7
[4 T ₁ +Rb ⁺] ₂ (dimeric T ₁ -tetramers)	1733.1	1735.2
[4 T ₁ +Rb ⁺]+[5 T ₁ +Rb ⁺]	1939.3	1941.8
5 T ₁ +Rb ⁺ (T ₁ -pentamer)	2144.9	2147.9
[5 T ₁ +Rb ⁺] ₂ (dimeric T ₁ -pentamers)	2144.9	2147.9
T ₁ +Cs ⁺	545.5	545.1
2 T ₁ +Cs ⁺	957.0	957.3
[2 T ₁ +Cs ⁺]+[3 T ₁ +Cs ⁺]	1163.3	1163.9
3 T ₁ +Cs ⁺	1368.4	1369.5
[3 T ₁ +Cs ⁺]+[4 T ₁ +Cs ⁺]	1575.2	1576.4
4 T ₁ +Cs ⁺ (T ₁ -tetramer)	1780.8	1782.7
[4 T ₁ +Cs ⁺] ₂ (dimeric T ₁ -tetramers)	1780.8	1782.7
[4 T ₁ +Cs ⁺]+[5 T ₁ +Cs ⁺]	1987.0	1989.3
5 T ₁ +Cs ⁺ (T ₁ -pentamer)	2192.1	2194.9
[5 T ₁ +Cs ⁺] ₂ (dimeric T ₁ -pentamers)	2192.6	2195.4

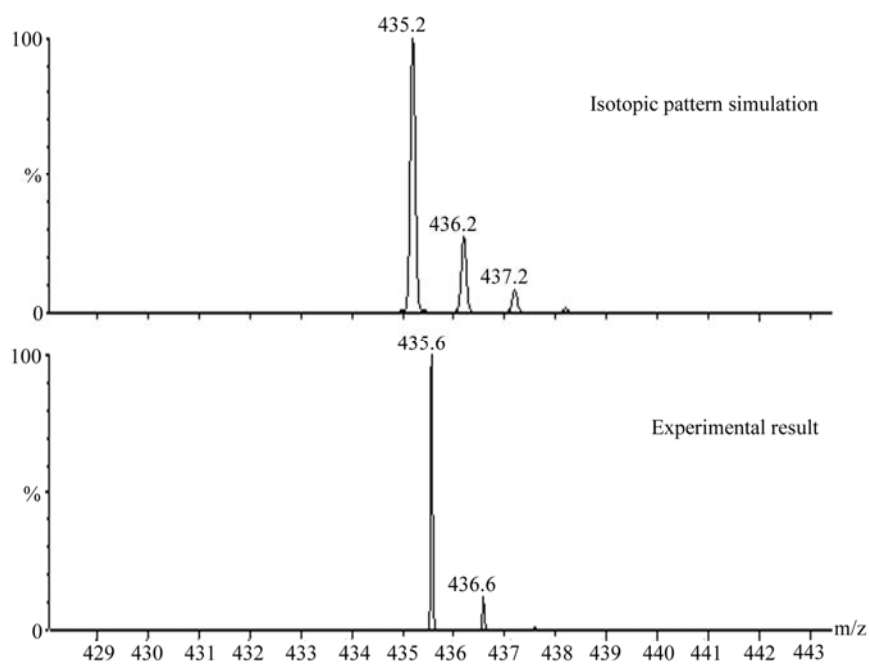


Figure S13. Comparison between experimental result and simulated isotopic pattern for TOF-ESI-MS of T_1+Na^+ ion.

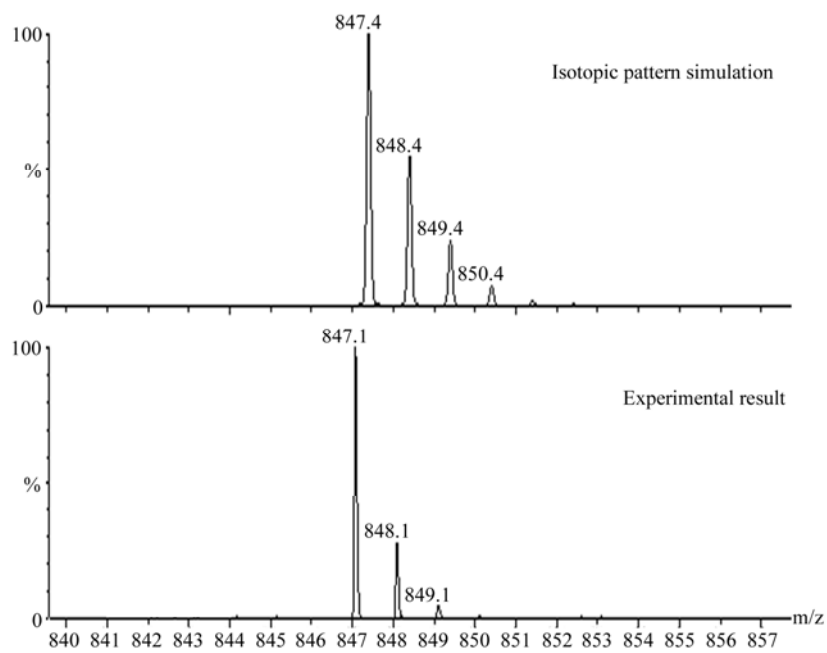


Figure S14. Comparison between experimental result and simulated isotopic pattern for TOF-ESI-MS of $2T_1+Na^+$ ion.

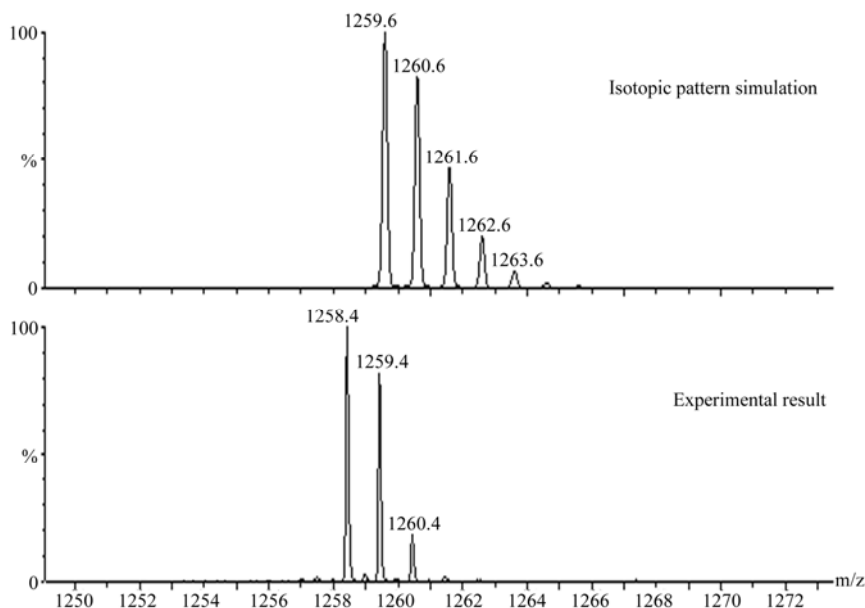


Figure S15. Comparison between experimental result and simulated isotopic pattern for TOF-ESI-MS of $3\mathbf{T}_1+\text{Na}^+$ ion.

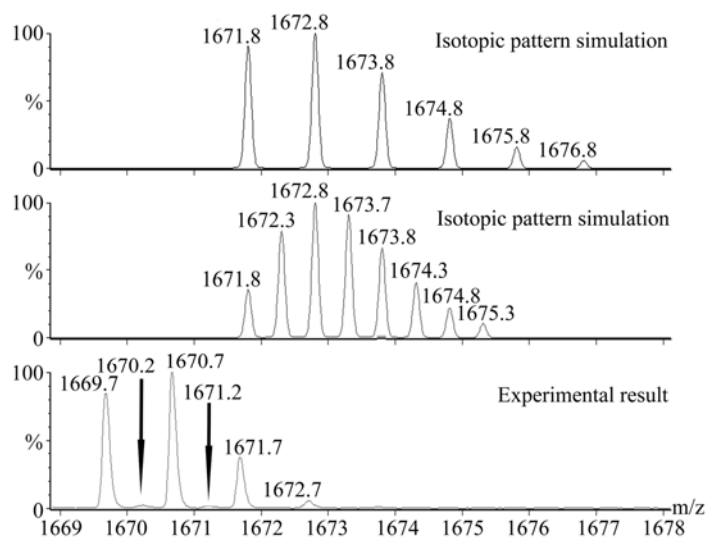


Figure S16. Comparison between experimental results and simulated isotopic patterns for TOF-ESI-MS of $4\mathbf{T}_1+\text{Na}^+$ monomer (\mathbf{T}_1 -tetramer) and $4\mathbf{T}_1+\text{Na}^+$ dimer (or dimeric \mathbf{T}_1 -tetramers). Top: isotopic pattern simulation for $4\mathbf{T}_1+\text{Na}^+$ monomer; Middle: isotopic pattern simulation for $4\mathbf{T}_1+\text{Na}^+$ dimer; Bottom: experimental results showing a combined signal of major $4\mathbf{T}_1+\text{Na}^+$ monomer and minor $4\mathbf{T}_1+\text{Na}^+$ dimer.

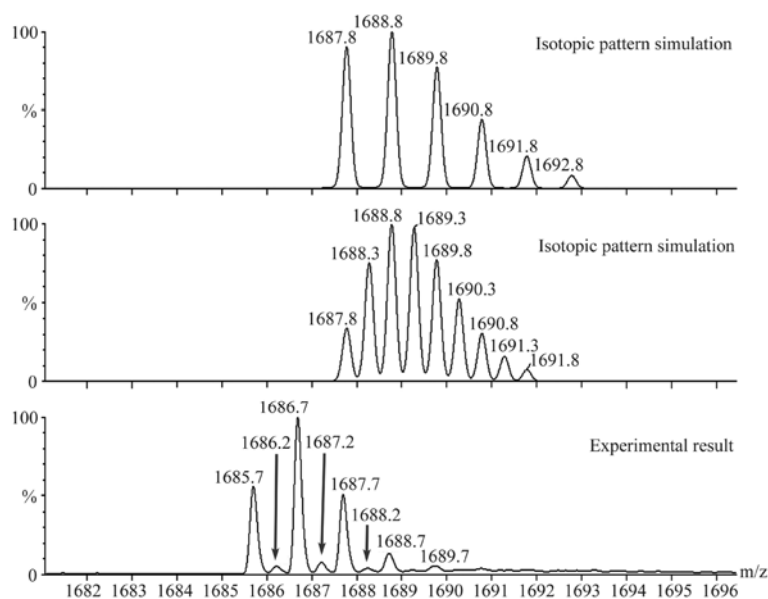


Figure S17. Comparison between experimental results and simulated isotopic patterns for TOF-ESI-MS of $4\mathbf{T}_1+\mathbf{K}^+$ monomer (\mathbf{T}_1 -tetramer) and $4\mathbf{T}_1+\mathbf{K}^+$ dimer (or dimeric \mathbf{T}_1 -tetramers). Top: isotopic pattern simulation for $4\mathbf{T}_1+\mathbf{K}^+$ monomer; Middle: isotopic pattern simulation for $4\mathbf{T}_1+\mathbf{K}^+$ dimer; Bottom: experimental results showing a combined signal of major $4\mathbf{T}_1+\mathbf{K}^+$ monomer and minor $4\mathbf{T}_1+\mathbf{K}^+$ dimer.

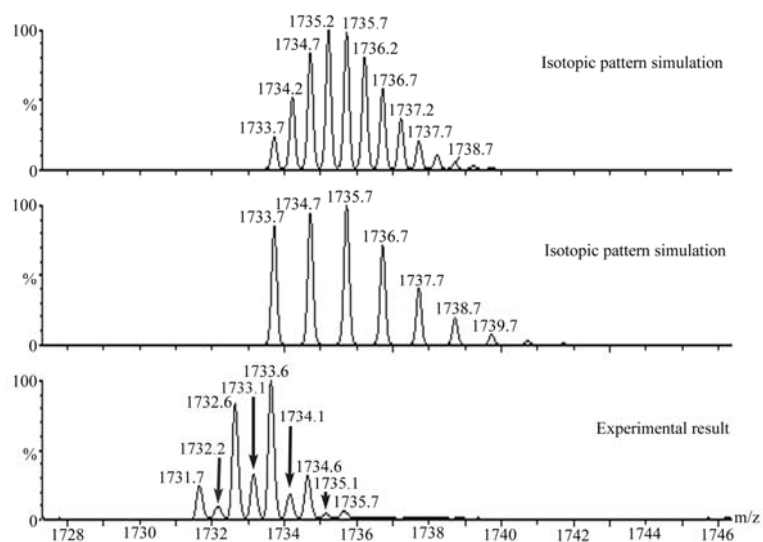


Figure S18. Comparison between experimental results and simulated isotopic patterns for TOF-ESI-MS of $4\mathbf{T}_1+\mathbf{Rb}^+$ monomer (\mathbf{T}_1 -tetramer) and $4\mathbf{T}_1+\mathbf{Rb}^+$ dimer (or dimeric \mathbf{T}_1 -tetramers). Top: isotopic pattern simulation for $4\mathbf{T}_1+\mathbf{Rb}^+$ dimer; Middle: isotopic pattern simulation for $4\mathbf{T}_1+\mathbf{Rb}^+$ monomer; Bottom: experimental results showing a combined signal of major $4\mathbf{T}_1+\mathbf{Rb}^+$ monomer and minor $4\mathbf{T}_1+\mathbf{Rb}^+$ dimer.

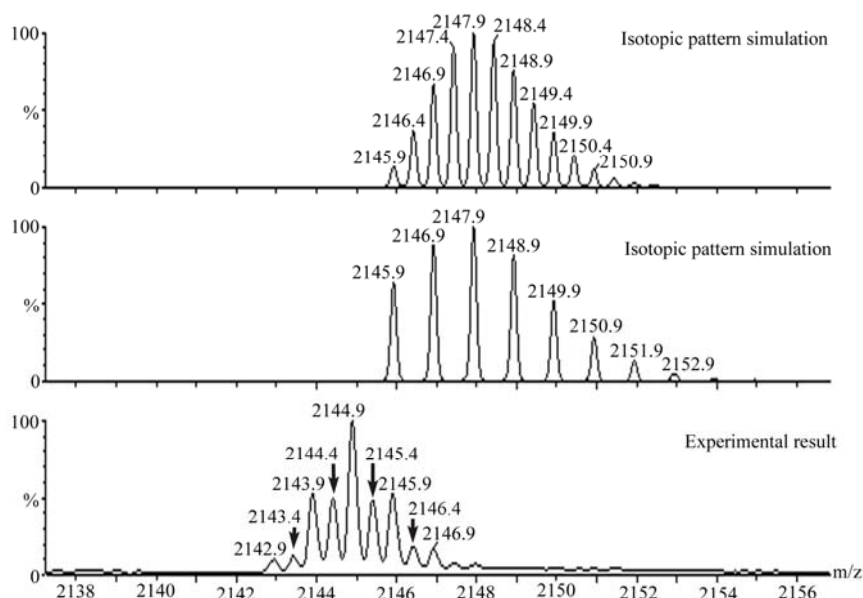


Figure S19. Comparison between experimental results and simulated isotopic patterns for TOF-ESI-MS of $5\mathbf{T}_1+\text{Rb}^+$ monomer (\mathbf{T}_1 -pentamer) and $5\mathbf{T}_1+\text{Rb}^+$ dimer (or dimeric \mathbf{T}_1 -pentamers). Top: isotopic pattern simulation for $5\mathbf{T}_1+\text{Rb}^+$ dimer; Middle: isotopic pattern simulation for $5\mathbf{T}_1+\text{Rb}^+$ monomer; Bottom: experimental result showing a combined signal of $5\mathbf{T}_1+\text{Rb}^+$ monomer and $5\mathbf{T}_1+\text{Rb}^+$ dimer.

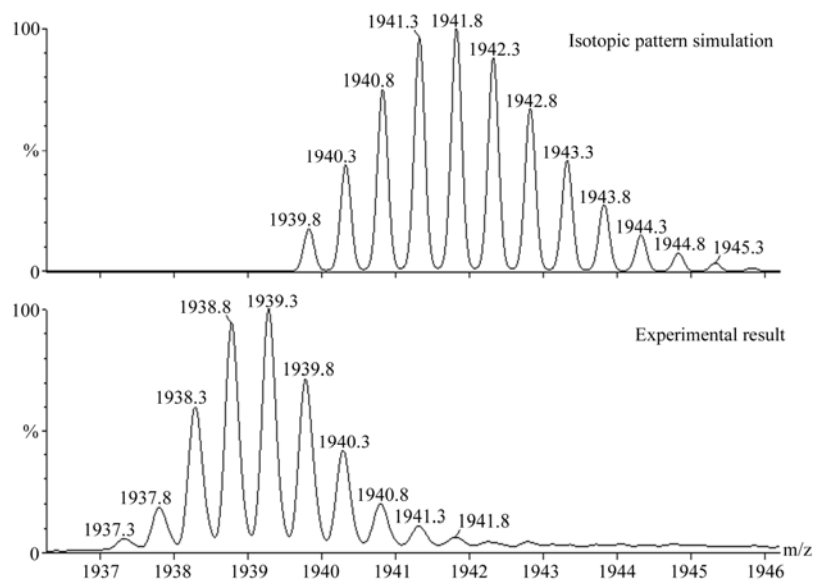


Figure S20. Comparison between experimental result and simulated isotopic pattern for TOF-ESI-MS of $[4\mathbf{T}_1+\text{Rb}^+]+[5\mathbf{T}_1+\text{Rb}^+]$ ion.

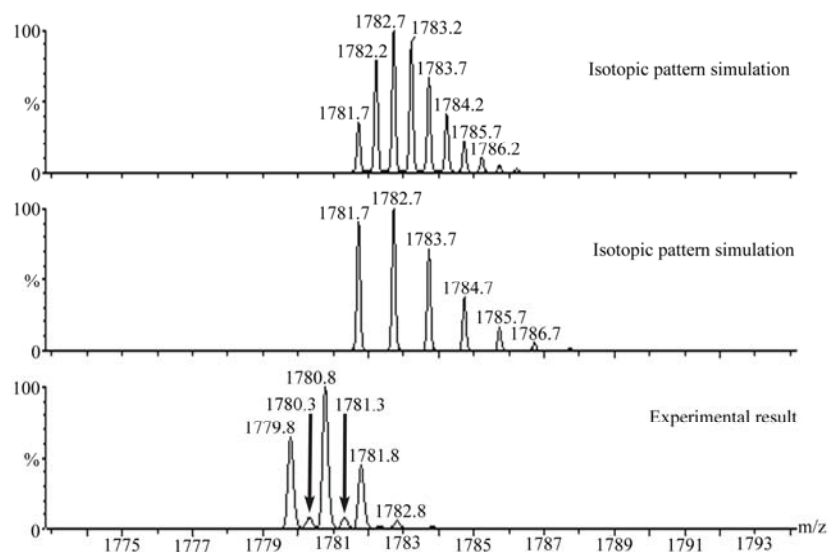


Figure S21. Comparison between experimental results and simulated isotopic patterns for TOF-ESI-MS of $4\mathbf{T}_1+\text{Cs}^+$ monomer (\mathbf{T}_1 -tetramer) and $4\mathbf{T}_1+\text{Cs}^+$ dimer (or dimeric \mathbf{T}_1 -tetramers). Top: isotopic pattern simulation for $4\mathbf{T}_1+\text{Cs}^+$ dimer; Middle: isotopic pattern simulation for $4\mathbf{T}_1+\text{Cs}^+$ monomer; Bottom: experimental results showing a combined signal of major $4\mathbf{T}_1+\text{Cs}^+$ monomer and minor $4\mathbf{T}_1+\text{Cs}^+$ dimer.

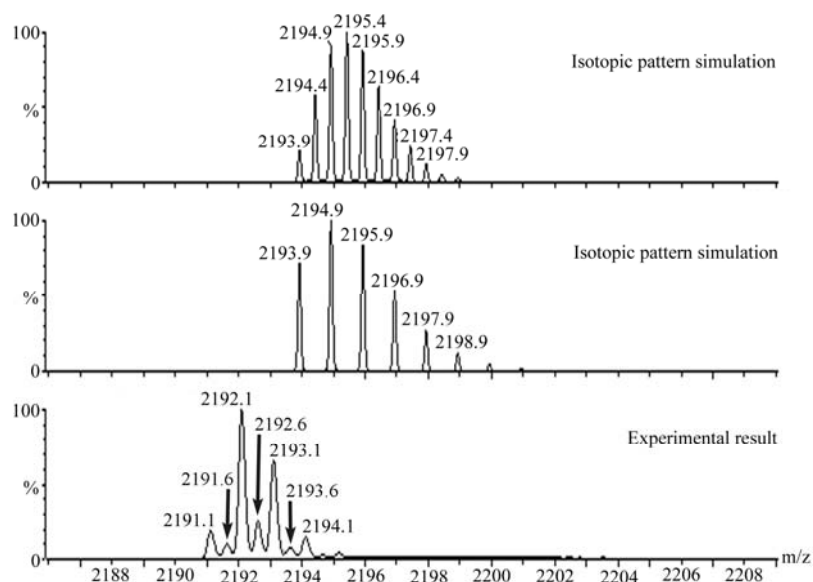


Figure S22. Comparison between experimental results and simulated isotopic patterns for TOF-ESI-MS of $5\mathbf{T}_1+\text{Cs}^+$ monomer (\mathbf{T}_1 -pentamer) and $5\mathbf{T}_1+\text{Cs}^+$ dimer (or dimeric \mathbf{T}_1 -pentamers). Top: isotopic pattern simulation for $5\mathbf{T}_1+\text{Cs}^+$ dimer; Middle: isotopic pattern simulation for $5\mathbf{T}_1+\text{Cs}^+$ monomer; Bottom: experimental results showing a combined signal of major $5\mathbf{T}_1+\text{Cs}^+$ monomer and minor $5\mathbf{T}_1+\text{Cs}^+$ dimer.

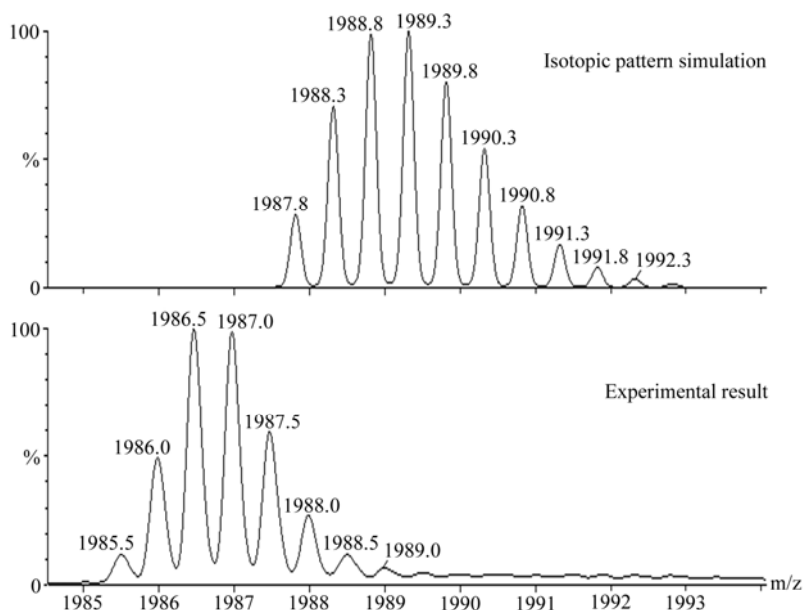


Figure S23. Comparison between experimental result and simulated isotopic pattern for TOF-ESI-MS of $[4\mathbf{T}_1+\text{Cs}^+]+[5\mathbf{T}_1+\text{Cs}^+]$ ion.

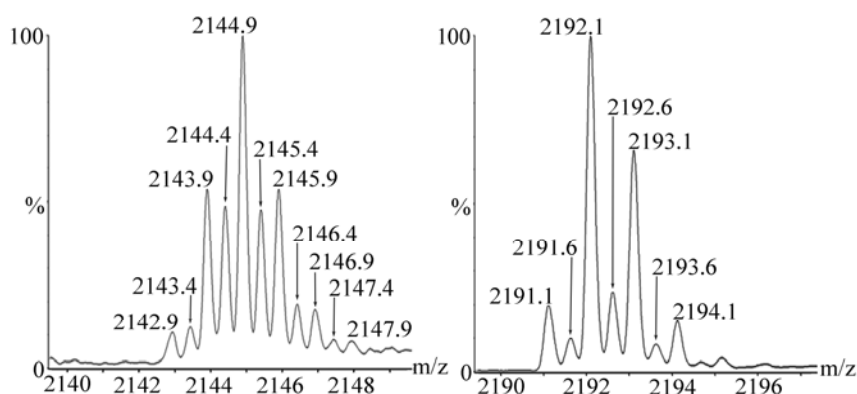


Figure S24. Positive ion-mode TOF-ESI-MS sections for \mathbf{T}_1 -pentamers and dimeric \mathbf{T}_1 -pentamers in acetonitrile. Left: combined signal of $5\mathbf{T}_1+\text{Rb}^+$ monomer and $5\mathbf{T}_1+\text{Rb}^+$ dimer; right: combined signal of major $5\mathbf{T}_1+\text{Cs}^+$ monomer and minor $5\mathbf{T}_1+\text{Cs}^+$ dimer.